Bioorganic & Medicinal Chemistry 25 (2017) 4297–4303

Contents lists available at ScienceDirect

Bioorganic & Medicinal Chemistry

journal homepage: www.elsevier.com/locate/bmc

Synthesis and characterization of monophosphinic acid DOTA derivative: A smart tool with functionalities for multimodal imaging

Satya Narayana Murthy Chilla [a,*], Ondrej Zemek [b], Jan Kotek [b], Sébastien Boutry [a,c], Lionel Larbanoix [a,c], Coralie Sclavons [a,c], Luce Vander Elst [a,c], Ivan Lukes [b], Robert N. Muller [a,c], Sophie Laurent [a,c,*]

[a] Department of General, Organic and Biomedical Chemistry, NMR and Molecular Imaging Laboratory, University of Mons, Avenue Maistriau, 19, Mendeleïev Building, 7000 Mons, Belgium
[b] Department of Inorganic Chemistry, Universita Karlova, Hlavova 2030, 128 40 Prague 2, Czech Republic
[c] Centre for Microscopy and Molecular Imaging (CMMI), Rue Adrienne Bolland, 8, 6041 Charleroi-Gosselies, Belgium

ARTICLE INFO

Article history:
Received 6 February 2017
Revised 30 May 2017
Accepted 8 June 2017
Available online 15 June 2017

Keywords:
Contrast agents
Macrocyclic ligands
Peptide conjugation
Gadolinium complex
Relaxivity

ABSTRACT

A new facile synthetic strategy was developed to prepare bifunctional monophosphinic acid Ln-DOTA derivatives, Gd-DO2AGAP^{NBn} and Gd- DO2AGAP^{ABn}. The relaxivities of the Gd-complexes are enhanced compared to Gd-DOTA. Monophosphinic acid arm of these Gd-complexes affords enhancement of inner sphere water exchange rate due to its steric bulkiness. The different functionalities of DO2AGAP^{NBn} were appended in trans positions and are designed to conjugate identical or different vectors according to the potential applications. The conjugation of Gd-DO2AGAP^{ABn} with E3 peptide known to target apoptosis was successfully performed and in vivo MRI allowed cell death detection in a mouse model.

1. Introduction

Magnetic resonance imaging (MRI) is an effective tool in biomedical research for understanding biological processes in living organisms as well as in clinical diagnosis due to its excellent spatial resolution, its non-invasiveness and its limitless tissue penetration. The resolution and tissue specificity can be further enhanced by paramagnetic lanthanide complexes due to their exceptional magnetic properties.[1] Nowadays, MRI contrast agents (CA) can provide detailed information at sub-cellular level resolution.[2] In multimodal imaging a single multimodal probe could be sufficient to address the same pharmacokinetics and co-localization of the signal in each modality, allowing the correlation of the information obtained by the different methods and avoiding multiple dose injections of agents.[3] However, the sensitivity of each modality can be different by several orders of magnitude and obtaining a single molecule efficient in each imaging modality is not trivial.

Gadolinium(III) complexes of polyaminopolycarboxylates are widely used as CA in MRI.[4] The efficacy of a paramagnetic CA is assessed by its relaxivity (r_1). Relaxivity enhancement can be achieved by fast water exchange rate (usually expressed as water residence time, τ_M) and slow molecular tumbling rates characterized by the rotational correlation time τ_R.[4,5] Most of the commercially used MRI contrast agents are low-molecular-weight compounds and generally have too fast molecular tumbling, i.e. short τ_R. In general, they have also a relatively slow water exchange rate[4] (e.g. τ_M^{310} of Gd-DOTA = 122 ns, (DOTA = 1,4,7,10-tetraazacyclododecane-1,4,7,10-tetraacetic acid).[6,7] It has been reported that increasing the negative charge of the complex and bulkiness around central metal atom facilitates the fast exchange of the coordinated water molecule due to sterical reasons.[4] Extensive research about the relationship between water exchange rates and solution structures have been related to the structural isomers of lanthanide(III) DOTA complexes. It is well-known that DOTA-like ligands wrap around a lanthanide(III) ion yielding two coordination geometries, namely square antiprismatic (SA) and twisted square-antiprismatic (TSA).[4,5,8] It was observed that the TSA isomers had 10–100 times faster exchange rate of the coordinated water molecule.[9] In general, increased steric repulsion around the paramagnetic center favors the TSA isomers.[2]

In the present work, we designed a suitable ligand for different modalities, the complexes of which can exhibit favorable

* Corresponding authors at: Department of General, Organic and Biomedical Chemistry, NMR and Molecular Imaging Laboratory, University of Mons, Avenue Maistriau, 19, Mendeleïev Building, 7000 Mons, Belgium (S. Laurent).
E-mail addresses: satya.chilla@umons.ac.be (S.N.M. Chilla), modrej@natur.cuni.cz (O. Zemek), sophie.laurent@umons.ac.be (S. Laurent).

http://dx.doi.org/10.1016/j.bmc.2017.06.008
0968-0896/

characteristics for both optical imaging and MRI techniques. This system consists of a kinetically inert macrocyclic ligand covalently linked to an aromatic phosphinate moiety. Through this approach, complexes suited for magnetic and optical imaging and with identical bio distributions could be used in MRI and optical imaging techniques and should enable better interpretation of in vivo molecular imaging experiments.[10] We prepared DO2AGAP^{NBn} (Scheme 1), a DOTA derivative with two different arms: *p*-nitro benzyl phosphinic acid and pentanedioic acid arms in trans-position. Consequently, the nitro group will serve as good precursor of amine function for further conjugation of the probe. The hexapeptide E3 was previously selected as a phosphatidylserine (PS)-specific peptide using the phage-display method.[11] PS is a membrane phospholipid that is externalized by cells undergoing apoptosis, which is a natural genetically programmed cell death process occurring in several normal (e.g. embryonic development), pathologic (e.g. neurodegeneration) or therapeutic (e.g. anti-cancer treatment) conditions.[12] Apoptosis can be induced in thymus by intra-peritoneal injection of the synthetic glucocorticoid dexamethasone (DEX).[13] This cell death model was set up in mice for preliminary MRI testing of the here-presented compounds, conjugated or not to the E3 peptide.

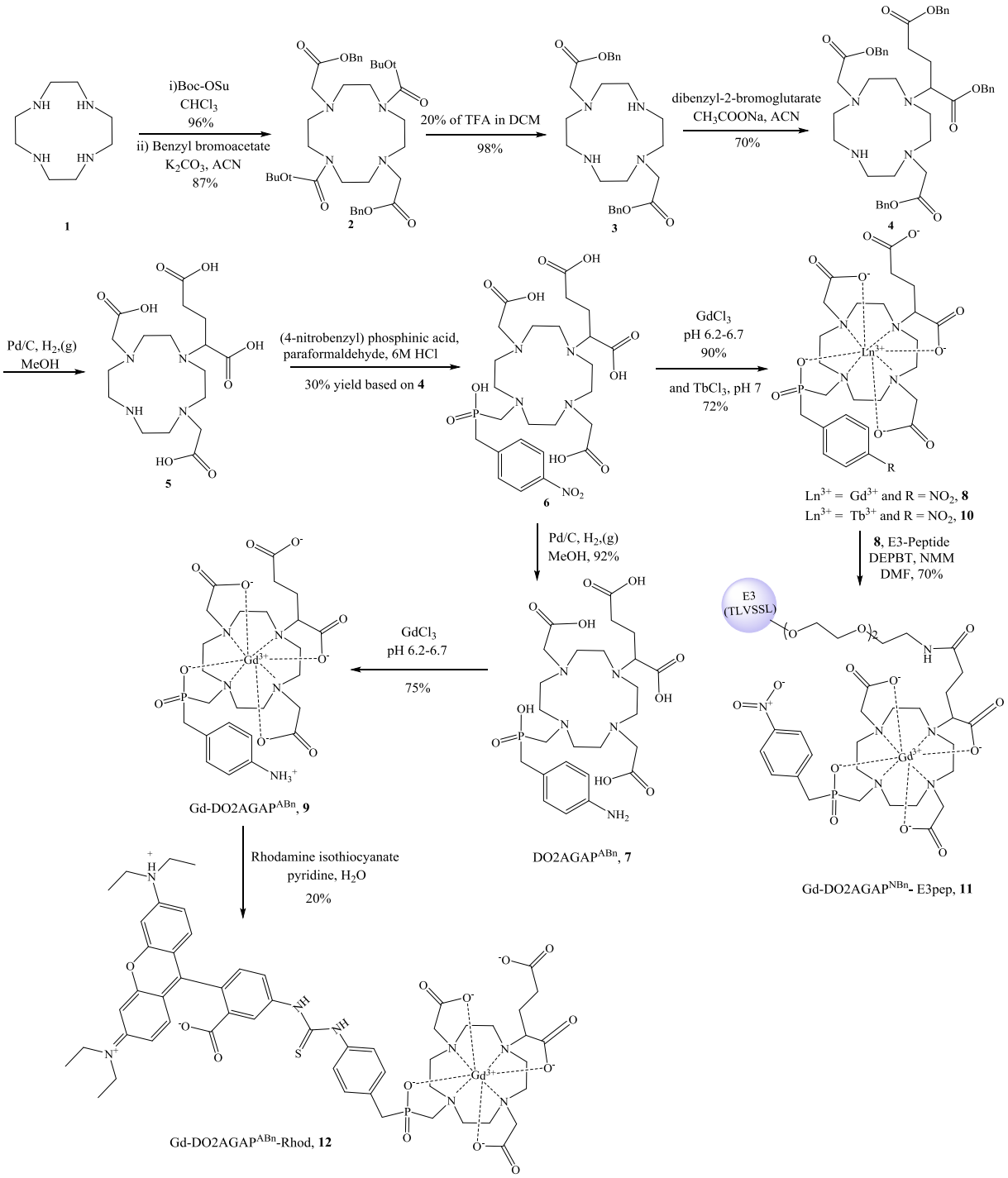

Scheme 1. Synthesis of monophosphinic acid derivatives and their conjugations with peptide and chromophore rhodamine isothiocyanate.

2. Results and discussion

2.1. Synthesis, complexation and conjugation of contrast agents

The controlled synthesis of ligand DO2AGAP^{NBn} **6** was obtained by a multi-step synthetic route starting from preparation of two pendant arms (Scheme 1). The key intermediates 4-nitrobenzylphosphinic acid[14] and dibenzyl 2-bromodipentanoate[15] were obtained according to literature procedures. The *trans*-DO2A **3** was synthesized by selective protection of nitrogen atoms *N-1* and *N-7* with Boc-O-succidimyl and further alkylation and deprotection as previously described.[16,17] Trialkylated product **4** was obtained by alkylating **3** with dibenzyl 2-bromopentanedioate in acetonitrile and sodium acetate used as a base. At this stage, we tried several bases for alkylation. Among them sodium acetate allowed to obtain a majority of trialkylated product even though we could not avoid the formation of minor tetraalkylated product. The second arm introduction was envisaged (after hydrogenolysis of compound **4** to intermediate **5**) by Mannich type reaction with formaldehyde and 4-nitrobenzylphosphinic acid in 6 N HCl, leading to the macrocyclic ligand **6** (DO2AGAP^{NBn}). As the secondary amine of **5** has low reactivity, a large excess of precursor and formaldehyde was used and in addition, a long reaction time was required. Ligand **6** DO2AGAP^{NBn} was isolated by ion exchange chromatography in good yields and the structure was confirmed by ^{1}H, ^{13}C, ^{31}P NMR and high-resolution mass spectrometry. Complexation of the ligand **6** DO2AGAP^{NBn} with Gd^{3+} or Tb^{3+} ions was performed under standard procedure. High-resolution mass spectrometry reveals peak corresponding to the molecular ion with the correct isotopic pattern for each complex. In order to prepare multimodal contrast agent, the conjugation efficiency of carboxylic acid of the Gd–DO2AGAP^{NBn} **8** complex was tested by using peptide-coupling reaction with a small hexapeptide under peptidic coupling methods at room temperature by using DEPBT and *N*-methyl morpholine (NMM) as a base. The compound **11** was obtained with good yield and purified by reverse phase chromatography. Our trials for conversion of nitro group of the compound **8** to amino group by catalytic hydrogenation were not successful. The ligand **6** was thus treated under hydrogenolysis to obtain **7** and Gd-DO2AGAP^{ABn} **9** was obtained after complexation in conditions similar to those used to complex **6**. Conjugation with rhodamine isothiocyanate depicted the availability of aniline group of complex **9** for further conjugations. The complex was purified by reverse phase chromatography and the corresponding mass confirms the formation of thiourea. (Scheme 1, see SI Fig. S1).

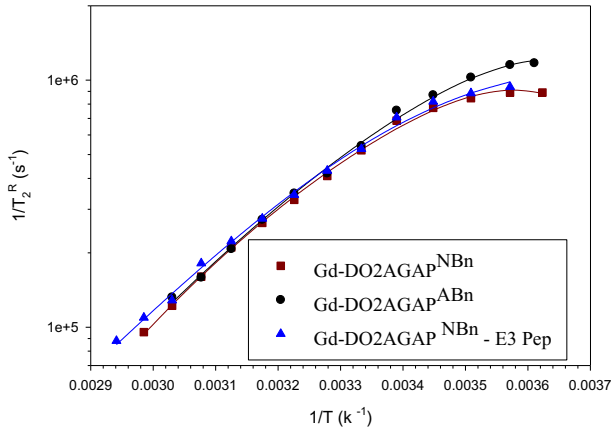

Fig. 1. Temperature dependence of the reduced transverse relaxation rate of ^{17}O at 11.75 T of Gd-DO2AGAP^{NBn} **8** (28.13 mM), Gd-DO2AGAP^{ABn} **9** (20.12 mM) and Gd-DO2AGAP^{NBn}-E3Pep **11** (26.032 mM).

2.2. Inner sphere hydration number (q) determination

A previous method for the determination of q by ^{17}O chemical shifts[18] used the dysprosium complexes, mainly because the contact contribution to its induced shift, is predominant as compared with its pseudo-contact shift and because Dy^{3+} causes a relatively small broadening of the ^{17}O signal. However, despite the quite large broadening of the ^{17}O signal induced by Gd^{3+}, this ion is better suited for such measurements since it induces only contact shift and no pseudo-contact shift. As previously reported,[19] we compared the ^{17}O chemical shift induced by the new Gd complex with well described Gd complexes, such as Gd–DOTA (Dotarem) and Gd–DTPA (Magnevist), for which $q = 1$ has been validated. The value obtained for Gd-DO2AGAP^{NBn} was estimated to be 0.74.

2.3. ^{17}O and ^{1}H NMRD measurements

The variable temperature dependence of the reduced ^{17}O transverse relaxation rates ($1/T_{2r}$) (Fig. 1) is typical of a water residence time lower than 100 ns at 310 K.[20] The observed τ_M values of Gd-DO2AGAP^{NBn} **8** and its derivatives (Table 1) show improvement compared to Gd-DOTA and to other phosphinate based DO3A complexes (Table 1).[14]

Proton relaxivity measurements in water revealed that the Gd-DO2AGAP^{NBn} **8** and its derivatives are stable in the pH range extending from 3 to 8. The magnetic field dependence of the proton longitudinal water proton relaxivities (r_1 NMRD profile) measured at 310 K shows higher relaxivities for our new complexes as compared to those of the parent compound Gd–DOTA.[20] At

Table 1
Parameters obtained from ^{17}O transverse relaxometry and ^{1}H NMRD of Gd-DO2AGAP^{NBn} **8**, Gd-DO2AGAP^{ABn} **9**, Gd-DO2AGAP^{NBn} – E3Pep **11** Gd-DO2AGAP^{ABn}-Rhod **12** and Gd-DOTA complexes in water at 37 °C.

Parameters	Gd–DO2AGAP^{NBn}[a] **8**	Gd–DO2AGAP^{ABn}[a] **9**	Gd–DO2AGAP^{NBn}–E3peptide[a] **11**	Gd-DO2AGAP^{ABn}-Rhod **12**	Gd–DOTA[a,b]
τ_M^{310} [ns]	20.3 ± 1.4	15.8 ± 0.1	10.8 ± 0.4	16[c]	122 ± 10
$\Delta H^{\neq}$ [kJ mol^{-1}]	62.6 ± 0.1	54.0 ± 0.1	44.9 ± 0.05	–	50.1 ± 0.2
$\Delta S^{\neq}$ [J mol^{-1} K^{-1}]	104.0 ± 0.3	78.5 ± 0.3	52.2 ± 0.2	–	48.7 ± 0.2
A/ħ [10^6 rad s^{-1}]	−2.90 ± 0.02	−2.8 ± 0.1	−2.82 ± 0.02	–	−3.42 ± 0.03
B [10^{20} s^{-2}]	16.2 ± 0.4	16.5 ± 0.5	8.2 ± 0.3	–	1.94 ± 0.09
τ_v^{298} [ps]	12.1 ± 0.37	18.4 ± 0.5	13.5 ± 0.6	–	11.4 ± 0.5
E_V [kJ mol^{-1}]	20.0 ± 12.4	20.0 ± 16.0	0.1 ± 13.3	–	4.0 ± 0.4
τ_v^{310} [ps]	13.6 ± 3.0	24.2 ± 5	17.2 ± 2.7	25.2 ± 2.1	7 ± 1
τ_R^{310} [ps]	77.3 ± 3.0	90.3 ± 2.4	115.3 ± 4.0	180 ± 4	53 ± 1
τ_{so} [ps]	247 ± 22	206 ± 10	202 ± 9	162 ± 3	404 ± 24

[a] The following parameters were fixed: (D is the diffusion coefficient = 3 · 10^{-9} m^2 s^{-1}, d is the distance of closest approach = 0.36 nm, r is the distance between the proton of the inner-sphere water molecule and Gd ion = 0.31 nm, q is fixed to 1 and τ_M was fixed to the value determined by ^{17}O NMR).
[b] Ref. 21c τ_M was fixed at the value obtained for Gd-DO2AGAP^{ABn} (16 ns).

60 MHz and 310 K, the relaxivities of Gd–DO2AGAP^{NBn} **8**, Gd–DO2AGAP^{ABn} **9** and Gd–DO2AGAP^{NBn}–E3Pep **11** are enhanced respectively by 39% (r_1 = 4.93 mM^{-1} s^{-1}), 56% (r_1 = 5.45 mM^{-1} s^{-1}) and 29% (r_1 = 4.28 mM^{-1} s^{-1}) as compared to Gd–DOTA (r_1 = 3.06 mM^{-1} s^{-1}).

The NMRD profiles were fitted using the inner sphere and outer sphere theories (Fig. 2). As expected, considering the molecular weight of Gd-DO2AGAP^{NBn} **8** and its derivatives, the value of τ_R is increased as compared to that of Gd-DOTA (Table 1). In addition, the temperature dependence of the proton longitudinal relaxivity at 20 MHz of complexes **8**, **9**, **11** and **12** confirms the fast water exchange for all the complexes (see SI Fig. S1). The r_1 value of Gd-DO2AGAP^{ABn} **9** at 25 °C and 20 MHz (r_1 = 7.2 s^{-1} mM^{-1}) is larger than the value reported for Gd-DO3AP^{ABn} at 25 °C and 10 MHz (6.7 s^{-1} mM^{-1})[14] as could be expected from the larger molecular weight of **9**. In addition, the τ_M^{298} values are in the same range, 16.2 ns for Gd-DO3AP^{ABn}[14] and 38 ns for Gd-DO2AGAP^{ABn} **9**.

2.4. ^{31}P NMR measurement

The interaction of the phosphinate with the Tb^{3+} center could be confirmed by ^{31}P NMR spectroscopy (Fig. 3). For the complex Tb-DO2AGAP^{NBn} **10**, two broad shifted peaks could be observed at a range of frequencies from 400 to 500 ppm. The direction and magnitude of the shifts are in agreement with what is observed for lanthanide complexes where the phosphinate group is in close proximity to the paramagnetic center. The two peaks corresponding to two isomeric forms SAP and TSAP of **10** are observed at ~468 ppm and ~413 ppm respectively with a 4:6 ratio. The large proportion of TSAP isomer is in good agreement with the fast water exchange of the Gd complex.

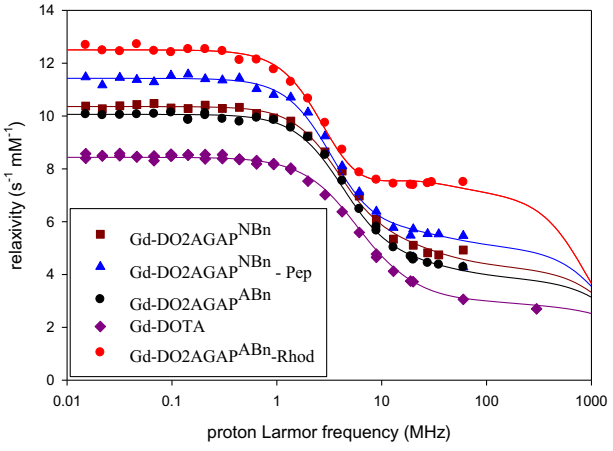

Fig. 2. ^{1}H NMRD relaxivity profiles of Gd–DO2AGAP^{NBn} **8**, Gd–DO2AGAP^{ABn} **9**, Gd–DO2AGAP^{NBn}–E3Pep **11** and Gd–DOTA in water at 37 °C.

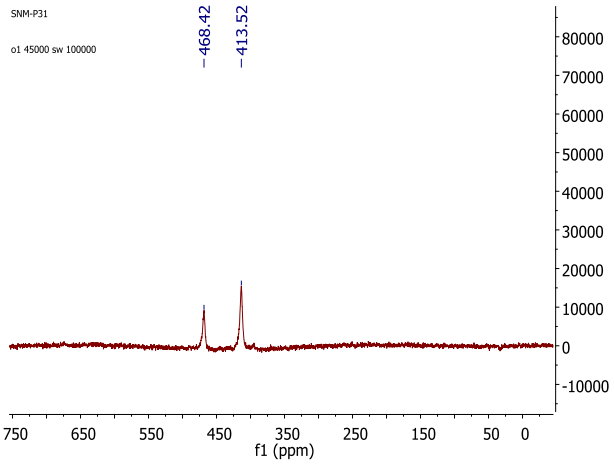

Fig. 3. ^{31}P spectrum of Tb–DO2AGAP^{NBn} **10** (D_2O).

2.5. Photophysical measurements

The emission experiments were performed in H_2O at 25 °C. After excitation of Tb-DO2AGAP^{NBn} **10** at 267 nm, no f-f transition of Tb^{3+} was observed showing no antenna effect probably because of the distance between the benzyl group and the central metal ion. In addition, the photo-physical properties of Gd-DO2AGAP^{ABn}–Rhodamine **12** was examined by recording the excitation and emission spectra of 1 mM solution in H_2O (see SI Fig. S2). For this complex a strong absorption could be observed at 556 nm and excitation at this wavelength resulted in broad emission band centered at 581 nm.

3. In vivo results

Thymus is a primary lymphoid organ in which T-lymphocytes (or T cells) develop for immune response capability. It is composed of an outer zone called cortex and an inner zone called medulla. T cell maturation (CD4+CD8+) from immature thymocytes occurs during their migration from cortex to medulla.[22] Dexamethasone (DEX) promotes thymocyte apoptosis and vessel permeability increase in the cortical region of thymus.[13,23] Immunohistochemistry of activated caspase-3 demonstrated ongoing apoptotic phenomenon in thymic cortex of mice 18 h after injection of DEX at a dose of 30 mg/kg (see SI Fig. S3). MRI showed signal intensity enhancement in thymic region corresponding to cortex in DEX-treated mice after injection of Gd-DO2AGAP^{NBn}-E3pep, suggesting specific targeting of PS on apoptotic thymocytes (see SI Fig. S3). Cortex/medulla signal intensity enhancement ratio was shown to be significantly increased ($p < 0.01$) in DEX-treated mice after injection of Gd-DO2AGAP^{NBn}-E3pep, regarding control groups (no DEX treatment + injection of Gd-DO2AGAP^{NBn}-E3pep or injection of Gd-DO2AGAP^{NBn} and DEX-treated + injection of Gd-DO2AGAP^{NBn}) (see Fig. 4 and SI Fig. S3).

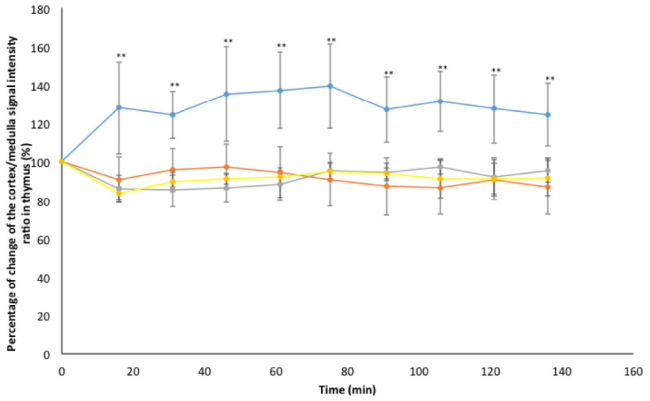

Fig. 4. Percentage of change of the cortex/medulla signal intensity ratio as a function of time after injection of Gd-DO2AGAP^{NBn}-E3pep in DEX-treated mice (n = 3, blue line), Gd-DO2AGAP^{NBn} in DEX-treated mice (n = 2, gray line), Gd-DO2AGAP^{NBn}-E3pep in untreated mice (n = 2, orange line), Gd-DO2AGAP^{NBn} in untreated mice (n = 2, yellow line). $^{**}p < 0.01$ for DEX-treated mice + Gd-DO2AGAP^{NBn}-E3pep regarding control groups.

4. Conclusion

In summary, a facile synthetic route was developed to prepare monophosphinic acid DOTA derivatives with two different functional groups such as carboxylic acid and nitro or amine. These new ligands DO2AGAP^{NBn} **6** and DO2AGAP^{ABn} **7** were easily complexed with lanthanides. Their relaxivities are enhanced due to the presence of phosphinic moiety that induces a τ_R increase and a significant molecular crowding which results in fast water exchange rates. The complexes were conjugated with small peptide on carboxylic acid arm or with a chromophore on amine of the phosphinate arm. Both functionalities were proved to be enough reactive to obtain multimodal contrast agent. The ^{31}P NMR of Tb–DO2AGAP^{NBn} **10** complex showed that the phosphinic acid moiety is coordinated to metal center but photophysical studies have not shown luminescence properties. In vivo experiments showed promising results in molecular MRI of cell death by conjugating PS-specific E3 hexapeptide to Gd-DO2AGAP^{NBn} **8** and targeting PS exposed by thymocytes in a mouse model of thymus cortex apoptosis induced by dexamethasone.

5. Experimental

5.1. General procedures

The chemicals were purchased from different companies: Acros, Aldrich, Fluka, Merck, Strem, Chematech, Polypeptide, TCI and VWR. All reagents were used without further purification. All solvents were distilled and/or dried prior to use by standard methodology except for those, which were reagent grades. Unless and otherwise mentioned, all the reactions were carried out under a nitrogen atmosphere and the reaction flasks were pre-dried by heat gun under vacuum. Pure water (18 MΩ cm^{-1}) was used throughout.[1,2] ^{1}H, ^{13}C and ^{31}P NMR spectra were recorded on Bruker 300 or 500 spectrometers. Chemical shift scale was referenced by following ways: ^{1}H – internal reference $CDCl_3$ at 7.27 ppm, MeOH at 3.33 ppm or D_2O at 4.75 ppm or TMS at 0.0 ppm; ^{13}C – internal reference $CDCl_3$ at 77.0 ppm, MeOH at 50 ppm or TMS at 0.0 ppm; ^{31}P – external reference 85% H_3PO_4 0.0 ppm and experiments were performed at 25 °C. ESI low-resolution mass spectra (ESI-MS) were recorded on Waters micromass ZQ system (Waters, Belgium) with full spectral detection mode in positive and negative ion modes. For HR-MS all experiments were performed on a Waters QToF 2 mass spectrometer. The analyte solutions (10^{-5} M methanol/water, 80:20) were delivered to the ESI source. Analytical thin layer chromatography (TLC) was performed on silica gel 60 F_{254} plates (E. Merck, Germany) using different mobile phases. The compounds were visualized by UV_{254} light and TLC plates were developed in Iodine chamber. The purification of the compounds was performed on KP-silica, KP-C_{18} cartridges from Biotage over Biotage flash chromatography instrument (Uppsala, Sweden) and by using silica gel 60 (70–230 mesh) from Merck. Reversed-phase analytical HPLC was performed in a stainless steel Xbridge (length 250 mm, internal diameter 4.6 mm, outside diameter 9.5 mm and particle size 5 μm) C18 column. Preparative HPLC was performed in a stainless steel Xbridge (length 250 mm, internal diameter 41.4 mm, outside diameter 50.8 mm and particle size 5 μm) C18 column (Varian). The compounds were purified using a gradient with the mobile phase starting from 95% solvent A (water) and 5% of solvent B (ACN) to 70% B in 10 min, 100% B in 18 min, 100% B isocratic till 24 min and decreased to 5% B in 28 min. The flow rate generally used for analytical HPLC was 1 mL/min and for preparative HPLC was 12 mL/min. All the solvents for HPLC were filtered through a Nylon-66 Millipore filter (0.45 μm) prior to use. Hexapeptide-E3 was synthesized on Liberty1 automated microwave peptide synthesizer with synthesis scale of 0.02–5 mmol by Fmoc chemistry. The microwave operating power was 120 V/60 Hz.

5.2. Synthetic procedures of the compounds

5.2.1. Di-tert-butyl 4-[2-(benzyloxy)-2-oxoethyl]-10-[(3-phenyl propanoyl)oxy]-1,4,7,10-tetraazacyclododecane-1,7-dicarbo-xylate (**2**)

To a solution of 1,4,7,10-tetraazacyclododecane free base **1** (714 mg, 4.067 mmol) in chloroform (35 mL), *N*-(*tert*-Butoxycarbonyloxy) succinimide (8.134 mmol) was added. The reaction mixture was stirred at room temperature for 28 h. Solvent was removed by rotary evaporation and 30 mL of NaOH 3 M was added to the remaining residue. The aqueous phase was extracted with chloroform (3.3 mL). The extracts were combined and dried (over K_2CO_3). The solvent was removed by rotary evaporation and the residue was dried in vacuum for several hours. 513 mg of the unpurified compound from the preceding reaction (1.3761 mmol) was solubilized in acetonitrile. 0.67 mL (2.87 mmol) of benzyl bromoacetate and 0.474 g (3.412 mmol) K_2CO_3 were added to this solution at room temperature, after which the mixture was heated under reflux for 8 h. The solids were discarded by filtration over Celite and the solvent was removed under *vacuum*. Chromatographic purification (alumina, 98/2 DCM/MeOH) yielded **2** as a slowly solidifying colourless oil (736 mg, 87% over all for two steps). ^{1}H NMR (500 MHz, $CDCl_3$) δ (ppm): 7.31 (m, 10H), 5.11 (s, 4H), 3.54 (s, 4H), 3.49 (m, 8H), 2.86 (m, 8H), 1.41 (s, br 18H). ^{13}C (500 MHz, $CDCl_3$) δ (ppm): 171.48, 157.11, 136.02, 79.33, 66.04, 55.04, 54.51, 46.68, 28.46. ESI-MS ($C_{36}H_{52}N_4O_8$); m/z = 668 $[M+H]^+$.

5.2.2. 2-(4,10-Bis-benzyloxycarbonylmethyl-1,4,7,10 tetraaza-cyclododec-1-yl)-pentanedioic acid dibenzyl ester (**4**)

Trifluroacetic acid (14 mL) was added to the solution of **2** (10.21 g, 0.015 mol) in dichloromethane (100 mL) and the mixture was stirred at room temperature for 16 h. The reaction mixture was evaporated under reduced pressure. Diethyl ether was used to precipitate the crude oil. The precipitate was washed with excess of ether followed by filtration and dried to obtain **3**. This product was directly used in the next step without further purification. 7.0 g (0.0149 mmol) of deprotected product and 2.64 g (0.03 mmol) of CH_3COONa were added to a solution of 5.8 g (0.015 mol) of dibenzyl 2-bromopentadioate in 100 mL of ACN and stirred for 48 h. The solid was discarded by filtration over a pad of Celite and the solvent was removed under reduced pressure to recover brownish oily crude mixture. Chromatographic purification (silica gel, 98/1.5/0.5 EtOAc/MeOH/TEA) of this mixture yielded **4** as slight yellow viscous oil. (8.1 g, 70%) ^{1}H NMR (300 MHz, $CDCl_3$) δ (ppm): 7.38–7.28 (m, 20H), 5.28–5.04 (m, 8H) 3.6–3.55 (m, 1H), 3.43 (s, br 4H), 3.1–3.0 (m, 6H), 2.6 (m, 4H), 2.52–2.5 (m, 6H), 2.22–1.97 (m, 4H). ^{13}C NMR (300 MHz, $CDCl_3$) δ (ppm): 177.75, 174.55, 172.8, 170.8, 135.73, 135.4, 128.72, 128.67, 128.59, 128.50, 128.45, 128.25, 128.17, 71.16, 67.16, 67.00, 66.54, 66.5, 59.89, 55.84, 55.21, 50.91, 49.60, 46.37, 30.59, 29.72, 26.18, 22.75, 20.52. ESI-MS ($C_{45}H_{54}N_4O_8$); m/z = 779 $[M+H]^+$.

5.2.3. 2-{4,10-Bis-carboxymethyl-7-[hydroxy-(4-nitrobenzyl) phosphinoy-lmethyl]1,4,7,10 tetraazacyclododec-1-yl}-pentanedioic acid (**6**)

10% Pd/C (1.0 g) was added to a solution of **4** (8.0 g, 0.01 mol) in MeOH (100 mL) and the resulting suspension was shaken for 4 h under H_2 atmosphere. After filtration of the suspension over a Celite pad and after evaporation of the solvent under reduced pressure, 3.2 g of **5** were obtained. The crude product (3.2 g, 8.13 mmol) was dissolved in 6 N HCl (20 mL). 1.95 g (0.065 mol) of paraformaldehyde and 6.5 g of 4-nitrobenzylphosphinic acid

(0.03 mol) were added to the latter solution and stirred at 50 °C for 2 days. Reaction mixture was cooled to 0 °C and all solvents were evaporated under vacuum. The product was purified using strong cation exchanger chromatography (Dowex 50, H^+-form, 6 × 25 cm, elution with water followed by 5% aq. ammonia). After evaporation of the solvents, the product was collected as a yellow oily NH_4^+-salt. The mixture was again subjected to anion exchanger (Dowex 5, Cl^- form, 15 × 3.8 cm elution with water 5% HCl). Evaporation of the solvents provided HCl salt of ligand. The chloride salt was dissolved in water, poured onto a column of a strong cation exchanger (Dowex 50, H^+-form, 4 × 25 cm) and the column was eluted with 10% aq. pyridine. After evaporation of the excess of pyridine from the eluate, the Hpy^+-salt was dissolved in a minimum amount of water and subjected to reverse phase flash chromatography, eluted with water/acetonitrile and yielded **6** (0.82 g, 30% based on **4**). ^{1}H NMR (500 MHz, D_2O) δ (ppm): 8.12–8.1 (d, J = 10 Hz, 2H), 7.43–7.41 (d, J = 10 Hz, 2H), 3.75–3.64 (m, 5H), 3.48–2.85 (m, 20H), 2.63–2.61 (m, 2H), 1.96 (s br, 2H). ^{13}C NMR (500 MHz, D_2O) δ (ppm): 177.3, 174.9, 173.5, 173.2, 146.5, 138.9, 131.1, 130.0, 122.1, 122.0, 66.5, 58.9, 58.2, 54.6, 54.1, 52.7, 52.4, 52.3, 51.1, 50.5, 41.2, 31.3, 30.2, 25.2. ^{31}P (500 MHz, D_2O) δ (ppm): 38.22 (S). HRMS (ESI): calcd for $C_{25}H_{38}N_5O_{12}P$; $[M+H]^+$ 632.2333; found 632.2334.

5.2.4. 2-{7-[(4-Aminobenzyl)hydroxyphosphinoylmethyl]-4,10-bis-carboxymethyl-1,4,7,10 tetraaza-cyclododec-1-yl}-pentanedioic acid (**7**)

10% Pd/C (0.1 g) was added to a solution of **6** (0.15 g, 0.23 mmol) in EtOH (10 mL) and the resulting suspension was shaken for 4 h under H_2 atmosphere. The suspension was filtered over a celite pad, and after evaporation of the solvent under reduced pressure **7** was obtained (0.13 g, 92%). ^{1}H NMR (500 MHz, D_2O) δ (ppm): 6.82–6.8 (d, J = 10 Hz, 2H), 6.33–6.3 (d, J = 10 Hz, 2H), 3.75–3.64 (m, 5H), 3.4–2.80 (m, 20H), 2.65–2.61 (m, 2H), 1.96 (s br, 2H). ^{13}C NMR (500 MHz, D_2O) δ (ppm): 177.3, 174.9, 173.5, 173.2, 145.5, 138.9, 138.3, 129.1, 116.1, 122.0, 66.5, 58.9, 58.2, 54.6, 54.1, 52.7, 52.4, 52.3, 51.1, 50.5, 41.2, 31.3, 30.2, 25.2. ^{31}P (500 MHz, D_2O) δ (ppm): 37.22 (s). ESI-MS ($C_{25}H_{40}N_5O_{10}P$); m/z = 602.6 $[M+H]^+$

5.3. Preparation of Gd^{3+} complex of DO2AGAP^{NBn} (**8**)

The complex was obtained by adding portion wise $GdCl_3{\cdot}6H_2O$ to a solution of **6** (0.26 g, 0.69 mmol) in H_2O (5 mL), maintaining the pH between 6.2 and 6.7 by addition of 1 N Pyridine. The final pH of the solution after stirring 24 h was 6.3. The excess of the free lanthanide was removed as $Gd(OH)_3$ precipitate, which appeared at pH 9. The resulting solution was treated with chelex-100 to remove free Gd^{3+} ions. The absence of free Gd^{3+} ions was confirmed by an Arsenazo III test[24] (in 0.1 M NaAc/HAc buffer solution, pH 5.2). The pH of the supernatant was decreased to 7 and the solution was freeze-dried. The complex was dissolved in water, purified by reverse phase flash chromatography and freeze-dried, yielding Gd–DO2AGAP^{NBn} (**8**) as a white powder (450 mg, 90%). The compound was purified by preparative HPLC as mentioned above. HPLC: R_t = 9.5 min, purity (215 nm): 96% HRMS (ESI): calcd for $C_{25}H_{34}GdN_5O_{12}P$; $[M+Na]^+$ 805.1126; found 805.1090.

5.4. Preparation of Gd^{3+} complex of DO2AGAP^{ABn} (**9**)

Gadolinium(III) complex of DO2AGAP^{ABn} was prepared by mixing a 1:1.1 M ratio of $GdCl_3{\cdot}6H_2O$ (0.054 g, 0.14 mmol) and ligand **7** (0.08 g 0.13 mmol) in water followed by addition of 1 N pyridine to adjust the pH to 7. The reaction mixture was briefly heated to 50 °C and then stirred at room temperature overnight. The complex was purified on Amberlite CG-50 with water elution. The solution was tested negatively for the presence of free lanthanide(III) ions by using arsenazo III test as an indicator (in 0.1 M NaAc/HAc buffer solution, pH 5.2). The complex was dissolved in water, purified by reverse phase flash chromatography and freeze-dried, yielding **Gd–DO2AGAP^{ABn}** as a pale off white powder (80 mg, 75%). The concentration of gadolinium(III) ions in solution was determined by relaxometric measurement. HRMS (ESI): calcd for $C_{25}H_{37}GdN_5O_{10}P$; $[M+Na]^+$ 775.1530; found 775.1534.

5.5. Preparation of Tb^{3+} complex of DO2AGAP^{NBn} (**10**)

Terbium(III) complex of DO2AGAP^{NBn} was prepared by mixing a 1:1.1 M ratio of $TbCl_3{\cdot}6H_2O$ (14.2 mg, 0.004 mmol) and ligand **6** (0.022 g, 0.004 mmol) in water followed by addition of 1 N pyridine to adjust the pH to 7. The reaction mixture was briefly heated to 50 °C and then stirred at room temperature overnight. The complex was purified on Amberlite CG-50 with water elution. The solution was tested for the absence of free lanthanide(III) ions by using arsenazo III test as an indicator (in 0.1 M NaAc/HAc buffer solution, pH 5.2). The complex was dissolved in water, purified by reverse phase flash chromatography and freeze-dried, yielding **Tb–DO2AGAP^{NBn}** as an off-white powder (20 mg, 72%). ESI-MS ($C_{25}H_{33}TbN_5O_{12}P2Na$); m/z = 832.2

5.6. Conjugation of peptide (E3) with Gd–DO2AGAP^{NBn} (**11**)

0.2 g (0.25 mmol) of **8** was dissolved in 5 mL of DMF to which 0.21 g (0.28 mmol) of peptide-E3, 89 mg (0.32 mmol) of DEPBT and 0.1 mL (0.752 mmol) of DIPEA were added. The reaction mixture was stirred for 4 h and diluted with 20 mL of water; a white precipitate was isolated by filtration and washed with ethyl acetate (50 mL). The solid was dried under reduced pressure and purified by semi-preparative HPLC using method A and obtained after 16 min of retention time. The compound was freeze-dried, and **11** was obtained as a white solid (0.27 g, 70%). HRMS (ESI): calcd for $C_{58}H_{93}GdN_{12}O_{24}P$; $[M+H]^+$ 1528.5398; found 1528.5422.

5.7. Conjugation of rhodamine with Gd-DO2AGAP^{ABn} (**12**)

32 mg of rhodamine isothiocyanate (0.072 mmol) and 6 μl of pyridine (0.07 mmol) were added to the aqueous solution of complex **9** (45 mg, 0.06 mmol) at room temperature. The mixture was stirred in the dark for 48 h. The mixture was freeze-dried and subjected to purification by reverse phase flash-chromatography over C18 silica gel using conditions as mentioned previously and **12** was obtained after 10 min of elution. (17 mg, 20%). ESI-MS ($C_{54}H_{65}GdN_8O_{13}PS$); m/z = 1274 $[M+Na]^+$.

5.8. ^{17}O NMR measurements and proton NMRD profiles

^{17}O NMR measurements were performed at 11.75 T on 350 μL samples contained in 5 mm o.d. tubes on a Bruker Avance 500 spectrometer (Karlsruhe, Germany). Temperature was regulated by air or nitrogen flow controlled by a Bruker BVT 3200 unit. ^{17}O transverse relaxation times of distilled water (pH 6.5–7) were measured using a CPMG sequence and a subsequent two-parameter fit of the data points. The 90° and 180° pulse lengths were 27.5 and 55 μs, respectively. The ^{17}O T_2 of water in complex solution was obtained from the line width measurements or CPMG sequence when linewidth was <80 Hz. All spectra were proton decoupled. The data are presented as the reduced transverse relaxation rate $\{1/T_2^r = 55.55/([\text{Gd-complex}]\times q \times T_2^p)$, where: [Gd complex] is the molar concentration of the complex, q is the number of coordinated water molecules and T_2^p is the paramagnetic transverse relaxation rate}. The fitting of the experimental data was performed as described in literature.[20,21] The gadolinium

concentration was determined by ICP-AES on a JobinYvon JY 70 instrument (Longjumeau, France) and was further confirmed by ^{1}H relaxometry of a decomplexed sample. Proton nuclear magnetic relaxation dispersion (NMRD) profiles were measured on a Stelar Spinmaster FFC (Mede, Italy) fast field cycling NMR relaxometer over a magnetic field range from 0.24 mT to 1.0 T. Measurements were performed on 0.6 mL samples contained in 10 mm o.d. Pyrex tubes. Additional relaxation rates at 20 and 60 MHz were obtained on a Minispec mq20 and a Minispec mq60, respectively.

5.9. In vivo MRI and image analysis

Animal experiments were performed under approval of the ethics committee of the Center for Microscopy and Molecular Imaging (CMMI protocol number 2012-06; LA1500589). Apoptosis was induced in thymus of 4–6 weeks old CD-1 female mice (Charles River (L'Arbresle, France)) by intraperitoneal injection of 30 mg/kg freshly prepared water-soluble dexamethasone (DEX, Sigma-Aldrich, Belgium, 25 mg/ml in PBS [Phosphate buffered saline] solution). For MRI observations, mice were anesthetized with isoflurane vaporized at 2–2.5% in O_2 à 2 L/min and placed in a warmed bed into the MRI scanner. Mice respiration was monitored during all experiment and anesthesia was adapted to 1.5–2% of isoflurane with O_2 flow of 0.4 L/min to maintain 20 respirations per minute. MRI was performed 16–18 h after dexamethasone injection, on a Bruker Biospec 9.4 T (Bruker, Karlsruhe, Germany). MR signal was detected using a volume coil (40 mm diameter) adapted for mouse body and connected to the animal bed. Images were acquired and visualized with the Paravision software (Bruker). The sequence used for this study was a T_1 spin-echo sequence (RARE): TR : 389.1 ms; TE: 8.9 ms; NEX (number of averages): 16; acquisition time: 14 min 56 s; matrix: 344 × 192; slice thickness: 1 mm; FOV: 3.2 × 1.8 cm; spatial resolution: 93 × 94 μm; fat saturation. Images were acquired on mice, treated with dexamethasone (developing apoptosis in the cortical region of thymus) and on control mice, up to 2 h (9 time points) after receiving an intravenous injection of Gd-DO2AGAP^{NBn}-E3pep or Gd-DO2AGAP^{NBn} (200 Â μmol Gd/kg). Image analysis was performed with the ImageJ software by measurement of a signal intensity enhancement ratio in thymus (cortex versus medulla), expressed as a percentage of change relative to the pre-contrast situation (considered as 100%). Statistical significance of differences between percentages of change were tested in Microsoft Excel using Student's *t*-test.

5.10. Immunohistochemistry

Mice were sacrificed in accordance with the ethics committee of CMMI (protocol 2012-06), 18 h after intraperitoneal injection of DEX (30 mg/kg). Thymus was collected and fixed in 4% formalin during 24 h. After PBS washing, tissue was dehydrated and embedded in paraffin using a Tissue-Tek VIP machine (Sakura Finetek, Japan). Thymus sections of 5-μm thickness were cut using a microtome and were automatically processed by a Discovery XT machine (Ventana/Roche, Belgium) for immunohistochemistry of activated (cleaved) caspase-3 enzyme. Sections were incubated at 37 °C for 1 h with anti-cleaved caspase-3 (Asp175) primary antibody (#9661, Cell Signaling, Netherlands), at dilution 1:100 in Ventana/Roche buffer, and for 24 min with secondary antibody (1:200; biotinylated anti-rabbit IgG made in goat (#BA-1000, Vector laboratories, LabConsult, Belgium)). Areas of caspase-3 activation were revealed by a streptavidin-biotin peroxidase detection system (Discovery DAB Map (#760-124, Ventana/Roche, Belgique)) allowing for diaminobenzidine precipitation at locations of antibody binding (brownish coloration) on thymic tissue. After nuclei coloration with hematoxylin, sections were dehydrated and mounted for light microscope observation.

Acknowledgements

The authors thank to the ARC Programs of the French Community of Belgium, UIAP VII program of Belspo, the Région Wallone (Gadolymph project n° 1317980 through the EuroNanoMed 2013 framework), Holocancer and Interreg programs**.** The support and sponsorship concerted by COST Actions TD1004 and EMIL program are acknowledged. The support from the Grant Agency of the Czech Republic (Project No. 16-03156S) is acknowledged. The authors thank the Center for Microscopy and Molecular Imaging (CMMI, supported by the Wallonia Region). The DIAPATH (Digital Image Analysis in Pathology) research unit of CMMI is thanked for immunohistochemical tissue processing.

A. Supplementary data

Supplementary data associated with this article can be found, in the online version, at http://dx.doi.org/10.1016/j.bmc.2017.06.008.

References

1. Merbach A, Helm L, Toth E. *The Chemistry of Contrast Agents in Medical Resonance Imaging*. 2nd ed. John Wiley & Sons Ltd; 2013.
2. (a) Webb AG. *J Magn Reson*. 2013;226:55–66;
(b) Di Corato R, Gazeau F, Le Visage C, et al. *ACS Nano*. 2013;9:7500–7512.
3. Frullano L, Meade T. *J Biol Inorg Chem*. 2007;12:939–949.
4. (a) Que EL, Chang CJ. *Chem Soc Rev*. 2010;39:51–60;
(b) Caravan P. *Chem Soc Rev*. 2006;35:512–523;
(c) Hermann P, Kotek J, Kubicek V, Lukes I. *Dalton Trans*. 2008;3027–3047.
5. (a) Tóth É, Pubanz D, Vauthey S, Helm L, Merbach AE. *Chem Eur J*. 1996;2:1607–1615;
(b) Caravan P, Ellison JJ, McMurry TJ, Lauffer RB. *Chem Rev*. 1999;99:2293–2352.
6. Powell DH, Dhubhghaill OMN, Pubanz D, et al. *J Am Chem Soc*. 1996;39:9333–9346.
7. Chilla SNM, Laurent S, Vander Elst L, Muller RN. *Tetrahedron*. 2014;70:5450–5454.
8. Aime S, Botta M, Fasano M, et al. *Inorg Chem*. 1997;36:2059–2068.
9. (a) Dunand FA, Aime S, Merbach AE. *J Am Chem Soc*. 2000;122:1506–1512;
(b) Woods M, Aime S, Botta M, et al. *J Am Chem Soc*. 2000;122:9781–9792;
(c) Woods M, Kovacs Z, Zhang S, Sherry AD. *Angew Chem Int Ed*. 2003;42:5889–5892.
10. Bonnet CS, Toth E. *C R Chim*. 2010;13:700–714.
11. Laumonier C, Segers J, Laurent S, et al. *J Biomol Screen*. 2006;11:537–545.
12. Elmore S. *Toxicol Pathol*. 2007;35:495–516.
13. (a) Brooks KJ, Bunce KT, Haase MV, et al. *Steroids*. 2005;70:267–272;
(b) Herold MJ, McPherson KG, Reichardt HM. *Cell Mol Life Sci*. 2006;63:60–72.
14. (a) Rudovsky J, Cigler P, Kotek J, et al. *Chem Eur J*. 2005;11:2373–2384;
(b) Rudovsky J, Kotek J, Hermann P, Lukes I, Mainero V, Aime S. *Org Biomol Chem*. 2005;3:112–117.
15. (a) Wardleworth PS, Baylis EK. EP 307362; 1989.;
(b) Dingwall JG, Ehrenfreund J, Hall RG. *Tetrahedron*. 1989;45:3787–3808.
16. Izatt RM, Pawlak K, Bradshaw JS, Bruening RL. *Chem Rev*. 1991;91:1721–2085;
(b) Burai L, Ren J, Kovacs Z, Brucher E, Sherry AD. *Inorg Chem*. 1998;37:69–75.
17. (a) Lowe MP, Parker D, Reany O, et al. *J Am Chem Soc*. 2001;123:7601–7609;
(b) Eisenwiener K-P, Powell P, Macke HR. *Bioorg Med Chem Lett*. 2000;10:2133–2135;
(c) Huskens J, Sherry AD, Torres DA, Kovacs Z, Andre JP, Geraldes CFGC. *Inorg Chem*. 1997;36:1495–1503.
18. Alpoim CM, Urbano AM, Geraldes CFGC, Peters JA. *J Chem Soc Dalton Trans*. 1992;463–467.
19. (a) Laurent S, Vander Elst L, Wautier M, Galaup C, Muller RN, Picard C. *Bioorg Med Chem Lett*. 2007;14:6230–6233;
(b) Granato L, Laurent S, Vander Elst L, Djanashvili K, Peters JA, Muller RN. *Contrast Media Mol Imaging*. 2011;6:482–491.
20. Vander Elst L, Maton F, Laurent S, Seghi F, Chapelle F, Muller RN. *Magn Reson Med*. 1997;38:604–614.
21. Laurent S, Vander Elst L, Muller RN. *Contrast Med Mol Imaging*. 2006;3:128–137.
22. Li L, Hsu HC, Grizzle WE, et al. *Immunology*. 2003;57:410–422.
23. Bubanovic IV. *Med Hypotheses*. 2003;60:315–320.
24. Rohwer H, Hoston E. *Anal Chim Acta*. 1997;3:271–277.